Available online at www.sciencedirect.com
SCIENCE DIRECT®
PERGAMON
International Journal of Heat and Mass Transfer 46 (2003) 3465–3475
International Journal of HEAT and MASS TRANSFER
www.elsevier.com/locate/ijhmt

Effect of the viscosity on the thermal transfer at early time to an impulsively started translating droplet

D. Léger *, R. Askovic

Laboratoire de Mécanique et d'Energétique, Université de Valenciennes et du Hainaut-Cambrésis (UVHC), Le Mont Houy, 59313 Valenciennes cedex 9, France

Received 10 December 2001; received in revised form 27 January 2003

Abstract

We study the effect of viscosity on the thermal transfer at the interface associated with a spherical liquid droplet impulsively started at constant velocity in another liquid of large extent at rest. Exact solutions for the thermal distributions are derived at short moving time. From algebraic and numerical considerations we show that viscous effects on the thermal transfer at the interface are negligible by comparison with the inviscid solutions. On the contrary, they predominantly occur on both side of it, in the two adjacent boundary layers, with a spreading effect with time.

Keywords: Thermal transfer; Droplets; Viscous effects

1. Introduction

A knowledge of the heat and also the mass transfer related to a moving droplet is of importance both for its fundamental interest and for technical applications in a number of industrial process such as conversion of saline to fresh water, for example. The aim of this paper is to analyze the effect of viscosity on the transient heat transfer associated with an impulsively translating droplet of a given liquid, moving at constant velocity in another liquid of large extent at rest. Our calculations are based on the thin boundary layer approximation, according to a perturbative scheme valid under the condition of sufficiently large Reynolds and Peclet numbers. Generally speaking, viscid effects are weak at large Reynolds numbers. However, it is not necessarily any more the case with more moderate *Re* values, still compatible with the thin boundary layer constraint. Then, their effect on the thermal transfer, namely their algebraic and numerical evaluation, and their localization in the interfacial region justifies the interest of this study. In this work, we assume that the droplet keeps its spherical shape, an assumption which will be examined later (Section 5). Moreover, we restrict our analysis to heat transfer at short time, i.e., when a well-defined dimensionless time variable τ is sufficiently small. In this limit, the energy conservation equation is solved analytically and exact expressions for the thermal distributions are derived. They are based on expansions of the thermal internal and external distributions on a set of Hermite polynomials. Our study is supplemented with a numerical evaluation of these solutions in two practical cases, namely droplets of *n*-pentane and carbon tetrachloride in water. The effect of viscosity on the heat transfer is finally discussed.

2. Pertubative scheme for the analysis of thermal boundary layers

We consider a spherical droplet of constant radius R, made of a given liquid having initially a uniform temperature T_0, impulsively being started at time $t = 0$ at constant velocity U_∞, in another liquid of infinite extent, initially at rest with a uniform temperature T_∞. For practical calculations, it is more convenient to consider

* Corresponding author.
E-mail address: daniel.leger@univ-valenciennes.fr (D. Léger).

0017-9310/03/$ - see front matter
doi:10.1016/S0017-9310(03)00127-3

Nomenclature

Pe	Peclet number	v	kinematic viscosity $= \frac{\mu}{\rho}$
Pr	Prandtl number	ρ	specific gravity
Re	Reynolds number	τ	dimensionless time $= \frac{U_\infty t}{R}$
R	droplet radius	σ	interfacial tension
T_0	initial temperature of the droplet	λ_{T_e}	$= \sqrt{\frac{Pre_e}{Re_e}}$
T_∞	temperature of the external liquid	λ_{T_i}	$= \sqrt{\frac{Pre_i}{Re_e}}$
U_∞	droplet velocity	β	$= \sqrt{\frac{k_e\rho_e c_{pe}}{k_i\rho_i c_{pi}}}$
c_p	specific heat	ξ	$= \sqrt{\frac{\mu_i\rho_i}{\mu_e\rho_e}}$
k	thermal conductivity		
e	subscript for the external liquid		
i	subscript for the internal liquid (droplet)		
κ	thermal diffusivity $= \frac{k}{\rho c_p}$		
μ	dynamic viscosity		

the reversed situation where the droplet is at rest in a liquid with a velocity $-U_\infty$ at large distance away from it. As previously mentioned, the shape of the droplet is assumed to remain unchanged as it moves. This assumption holds provided that Reynolds numbers are not too large ($Re \lesssim 500$) and that the interfacial tension σ is sufficiently large [1]. These constraints will be reexamined in Section 5. Following a procedure suggested by Boltze in his study of boundary layers over a body of revolution, we introduce a curvilinear system of coordinates [2] as shown in Fig. 1. We denote by $x = R\theta$ the arc length measured along any meridian from the front stagnation point, and y the coordinate normal to the droplet surface, taken outward as positive. In this work, the internal and external fluids will be referenced by the subscripts i and e respectively. Each of them is characterized by its specific gravity ρ, specific heat c_p, thermal conductivity and diffusivity, k and $\kappa = k/\rho c_p$ respectively, dynamic and kinematic viscosity, μ and $v = \mu/\rho$, respectively. For each of them, the relevant dimensionless numbers are the Reynolds number $Re = 2RU_\infty/v$, the Peclet number $Pe = 2U_\infty R/\kappa$, and finally the Prandtl number $Pr = v/\kappa \equiv Pe/Re$.

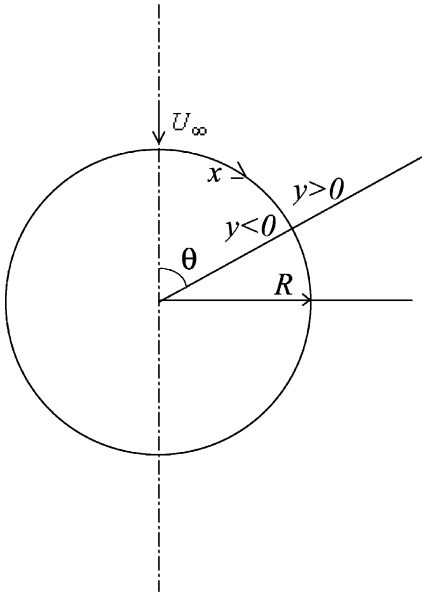

Fig. 1. Curvilinear system of coordinates at the spherical interface.

On the basis of the main following assumptions: (a) fully developed internal circulation, (b) inviscid flow fields (i.e., large Reynolds numbers) and, (c) thin thermal boundary layers (i.e., large Peclet numbers), then Chao [3] has shown that the transient internal and external thermal distributions express exactly as:

$$\frac{T_e - T_\infty}{T_0 - T_\infty} = \frac{1}{1+\beta}\operatorname{erfc} w_e, \quad \text{for } y \geqslant 0 \tag{1a}$$

$$\frac{T_i - T_\infty}{T_0 - T_\infty} = 1 - \frac{\beta}{1+\beta}\operatorname{erfc} w_i, \quad \text{for } y \leqslant 0 \tag{1b}$$

Here, $\operatorname{erfc} u = (2/\sqrt{\pi})\int_u^\infty \exp(-z^2)\,dz$ stands for the complementary error function [4], $\beta = ((k_e\rho_e c_{pe})/(k_i\rho_i c_{pi}))^{1/2}$ and the dimensionless variables w_e and w_i are defined as:

$$w_{e,i} = \frac{1}{2}\left(\frac{Pe_{e,i}}{\gamma}\right)^{1/2}\frac{|y|}{R} \tag{2}$$

with

$$\gamma = \frac{4}{3}\frac{\zeta}{\sin^4\theta} \tag{3}$$

$\zeta(\theta,\tau)$ is a function of $\cos\theta$ and the dimensionless time variable [1] $\tau = U_\infty t/R$, defined as [3]:

[1] In Chao's original paper [3], the dimensionless time variable is defined as $\tau = \kappa_e t/R^2$ with $(3/2)Pe_e\tau = 3(U_\infty t/R)$.

$$\zeta = (f - \cos\theta) - \tfrac{1}{3}(f^3 - \cos^3\theta) \tag{4}$$

where

$$f = \frac{1 + \cos\theta - (1 - \cos\theta)\exp(-3\tau)}{1 + \cos\theta + (1 - \cos\theta)\exp(-3\tau)} \tag{5}$$

For well-defined initial and boundary conditions supemented with conditions at the interface (see Section 4), Eqs. (1a) and (1b) are the solutions of the energy equation for the thermal external and internal boundary layers:

$$\frac{\partial T_{\mathrm{e,i}}}{\partial t} + \mathbf{U}_{\mathrm{e,i}} \cdot \nabla T_{\mathrm{e,i}} = \kappa_{\mathrm{e,i}} \frac{\partial^2 T_{\mathrm{e,i}}}{\partial y^2} \tag{6}$$

where $\nabla = \left(\frac{\partial}{\partial y}, \frac{1}{R}\frac{\partial}{\partial \theta}\right)$ stands for the gradient operator expressed in the curvilinear coordinates detailed above, and $\mathbf{U}_{\mathrm{e,i}} = (U_r, U_\theta)_{\mathrm{e,i}}$ is the inviscid flow field vector. The radial and circumferential velocity component, $U_{r(\mathrm{e,i})}$ and $U_{\theta(\mathrm{e,i})}$, of the external and internal flow fields are well known. The latter was first given by Hill [5]. Owing to the thin boundary layer approximation, valid whenever $|y|/R \ll 1$, they are approximated as:

$$U_{r\mathrm{e}} = -U_{r\mathrm{i}} = -3U_\infty \frac{|y|}{R}\cos\theta \tag{7a}$$

$$U_{\theta\mathrm{e}} = U_{\theta\mathrm{i}} = \tfrac{3}{2}U_\infty \sin\theta \tag{7b}$$

In this work, our main objective is to evaluate the resulting effect of the viscosity of both fluids on the transient thermal distributions at and in the vicinity of the interface. To do so, we first start splitting the thermal and flow fields distributions as:

$$T_{\mathrm{e,i}} = \overline{T}_{\mathrm{e,i}} + \widetilde{T}_{\mathrm{e,i}} \tag{8a}$$

$$\mathbf{U}_{\mathrm{e,i}} = \overline{\mathbf{U}}_{\mathrm{e,i}} + \widetilde{\mathbf{U}}_{\mathrm{e,i}} \tag{8b}$$

The first ones, adorned with a bar on the top, correspond to Chao's solutions (1a) and (1b) for the thermal distributions and to solutions (7a) and (7b) for the flow fields. The second one, adorned with a tilde on the top, stands for complemented contributions to these flows concerned with viscid effects.

Putting expressions (8a) and (8b) in Eq. (6) provides the required differential equations for the thermal distributions $\widetilde{T}_{\mathrm{e,i}}$. These equations get simplified when making use of a perturbative scheme for their resolution. For that purpose, we look at the predominant contributions in the convective term $\mathbf{U} \cdot \nabla T$. For the sake of simplicity, the internal and external cases will not be distinguished in what follows.Then, postulating that $\widetilde{U}_r$, $\widetilde{U}_\theta$, and $\widetilde{T}$ may be expanded according to the increasing powers of small parameters, namely λ_r, λ_θ and λ_T, and noting that $\partial/\partial y$ and $(1/R)(\partial/\partial\theta)$ when acting as differential operators on a function of the w variable (Eq. (2)) yield contributions of order $\sim(\sqrt{Pe}/R)$ and $(\sqrt{Pe}/R)(|y|/R)$ respectively, it is easily shown that each term in $\mathbf{U}\cdot\nabla T$, in unit $((U_\infty(T_0 - T_\infty))/R$, is of order: $\widetilde{U}_r(\partial\overline{T}/\partial y) \sim \lambda_r\sqrt{Pe}$, then $\overline{U}_r(\partial\widetilde{T}/\partial y) \sim \lambda_T(|y|/R)\sqrt{Pe}$, then $(\widetilde{U}_\theta/R)(\partial\overline{T}/\partial\theta) \sim \lambda_\theta\sqrt{Pe}(|y|/R)$ and finally $(\overline{U}_\theta/R)(\partial\widetilde{T}/\partial\theta) \sim \lambda_T\sqrt{Pe}(|y|/R)$. So it follows from this analysis that in the thin boundary limit approximation, i.e., when $|y| \ll R$ and more precisely $(|y|/R) \ll (1/\sqrt{Pe})$, the leading term in $\mathbf{U}\cdot\nabla T$ is just $\widetilde{U}_r\frac{\partial\overline{T}}{\partial y}$. The other remaining terms can be neglected and we conclude that the viscid contributions $\widetilde{T}_{\mathrm{e,i}}$ to the thermal distribution are also of order $\lambda_T \sim \lambda_r\sqrt{P_{\mathrm{e}}}$. So the perturbative scheme under consideration is also valid whenever $\lambda_T \sim \lambda_r\sqrt{P_{\mathrm{e}}} \ll 1$, a condition which will be reexamined later. Neglecting finally the quadratic contribution $\widetilde{\mathbf{U}}\cdot\nabla\widetilde{T}$ in the convective term provides the required equations for the $\widetilde{T}_{\mathrm{e,i}}$'s, at lowest order in the small λ_T parameters:

$$\frac{\partial\widetilde{T}_{\mathrm{e,i}}}{\partial t} + \widetilde{U}_{r(\mathrm{e,i})}\frac{\partial\overline{T}_{\mathrm{e,i}}}{\partial y} = \kappa_{\mathrm{e,i}}\frac{\partial^2\widetilde{T}_{\mathrm{e,i}}}{\partial y^2} \tag{9}$$

Next in Eq. (9), we take for $\widetilde{U}_{r(\mathrm{e,i})}$ and $\widetilde{U}_{\theta(\mathrm{e,i})}$ the exact expressions of the flow fields recently derived by one of us [6], also in the thin boundary layer approximation according to a perturbative scheme:

$$\frac{\widetilde{U}_{r(\mathrm{e,i})}}{U_\infty} = s_{\mathrm{e,i}}\frac{2\lambda_{r(\mathrm{e,i})}}{1+\xi}\left\{-6\gamma\cos\theta\left[i^2\mathrm{erfc}\ u_{\mathrm{e,i}} - \frac{1}{4}\right] + \mathrm{erf}\ u_{\mathrm{e,i}}\left[1 - 3\gamma\cos\theta - \left(\frac{1+f}{1+\cos\theta}\right)^4 \mathrm{e}^{-6\tau}\right]\right\} \tag{10a}$$

$$\frac{\widetilde{U}_{\theta(\mathrm{e,i})}}{U_\infty} = -\frac{3\lambda_{\theta(\mathrm{e,i})}}{1+\xi}\gamma^{1/2}\sin\theta\,\mathrm{ierfc}\ u_{\mathrm{e,i}} \tag{10b}$$

These expressions hold both for the internal and external flow subject to take the $s_{\mathrm{e,i}}$ sign in (10a) as $s_{\mathrm{e}} = +1$ and $s_{\mathrm{i}} = -1$. The ξ variable stands for $\xi = (\mu_{\mathrm{i}}\rho_{\mathrm{i}}/\mu_{\mathrm{e}}\rho_{\mathrm{e}})^{1/2}$, and the parameters $\lambda_{r(\mathrm{e,i})}$ and $\lambda_{\theta(\mathrm{e,i})}$ are defined as:

$$\lambda_{r\mathrm{e}} = \frac{1}{Re_{\mathrm{e}}}, \quad \lambda_{r\mathrm{i}} = \frac{1}{\sqrt{Re_{\mathrm{e}}Re_{\mathrm{i}}}}, \quad \lambda_{\theta\mathrm{e}} = \frac{1}{\sqrt{Re_{\mathrm{e}}}}, \quad \lambda_{\theta\mathrm{i}} = \frac{1}{\sqrt{Re_{\mathrm{e}}}} \tag{11}$$

They play the role of small expansion parameters in the perturbative scheme of the flow fields, as previously mentioned. Making use for the sake of simplicity of a common notation both for external and internal flows, we note that $\lambda_r \sim (1/Re)$, from which it follows $\lambda_T \sim (\sqrt{Pe}/Re)$. Then, the perturbative scheme for the thermal problem, as discussed above, holds provided $\lambda_T \sim (\sqrt{Pe}/Re) \ll 1$. Owing to the fact that $Pr \equiv (Pe/Re)$, this finally leads to the conditions $\lambda_{T_{\mathrm{e}}} \sim (Pr_{\mathrm{e}}/Re_{\mathrm{e}})^{1/2} \ll 1$ for the external case and $\lambda_{T_{\mathrm{i}}} \sim (Pr_{\mathrm{i}}/Re_{\mathrm{e}})^{1/2} \ll 1$ for the internal one.

In expressions (10a) and (10b), the dimensionless u_e and u_i variables are linked to the w_e and w_i's ones (Eq. (2)) by:

$$u_{e,i} = \frac{w_{e,i}}{\sqrt{Pr_{e,i}}} \tag{12}$$

They appear in Eqs. (10a) and (10b) as arguments of functions i^nerfc u (where n = integer, and ierfc $u \equiv i^1$erfc u) which correspond to the successive definite integrals [4] of the complementary error function erfc $u = 1 - \text{erf}\ u$.

Let us finally mentioned that contributions to the thermal distributions derived solving Eq. (9) for the $\widetilde{T}'_{e,i}$'s are closely related to dissipation due to the viscosity. In Eq. (9), viscid effect are contained within the flow fields (10a) and (10b) through the parameters defined in Eq. (11) which are proportional to the viscosity of the liquids. These flow fields themselves were deduced solving the Navier–Stokes equation for both the internal and external fluid according a perturbative scheme [6], and the viscid contribution $\sim\lambda_{r(e,i)} \sim Re$ originates from the dissipative term $\sim\nu\Delta\widetilde{U}$ in these equations.

3. Small time solutions for the thermal problem

Eq. (9) supplemented with (10a) and (10b) cannot be a priori solved analytically, at least at any time, but only numerically. The results of this study will be detailed in a forthcoming paper. In the present work, our main objective is to get quantitative and *algebraic* results for the viscid effects on the thermal transfer, namely, to give us some ideas as regards size. For that purpose, we restrict our analysis to the study of transfer at short time $\tau = U_\infty t/R \to 0$. As shown in Appendix A, the governing Eq. (9) can be solved analytically in that limit. Chao's solutions (1a) and (1b) take then the form:

$$\overline{T}_e^{(0)} = \lim_{\tau\to 0}\overline{T}_e = T_\infty + \frac{T_0 - T_\infty}{1+\beta}\text{erfc}\ w_e^0 \tag{13a}$$

$$\overline{T}_i^{(0)} = \lim_{\tau\to 0}\overline{T}_i = T_0 - \frac{\beta}{1+\beta}(T_0 - T_\infty)\text{erfc}\ w_i^0 \tag{13b}$$

with, owing to the fact that $\lim_{\tau\to 0}\gamma = 2\tau$:

$$w_{e,i}^0 = \lim_{\tau\to 0} w_{e,i} = \frac{1}{2}\left(\frac{Pe_{e,i}}{2\tau}\right)^{1/2}\frac{|y|}{R} \equiv \frac{|y|}{2\sqrt{\kappa_{e,i}t}} \tag{14}$$

One immediately get from (12):

$$u_{e,i}^0 = \lim_{\tau\to 0} u_{e,i} = \frac{1}{2}\left(\frac{Re_{e,i}}{2\tau}\right)^{1/2}\frac{|y|}{R} = \frac{|y|}{2\sqrt{\nu_{e,i}t}} \tag{15}$$

In a similar way, the expressions (10a) and (10b) for the flow fields reduce to

$$\widetilde{U}_{r(e,i)}^0 = \lim_{\tau\to 0}\widetilde{U}_{r(e,i)} = -24 s_{e,i}\frac{U_\infty\lambda_{r(e,i)}}{1+\xi}\ \tau\cos\theta\left[i^2\text{erfc}\ u_{e,i}^0 - \frac{1}{4}\right] \tag{16a}$$

$$\widetilde{U}_{\theta(e,i)}^0 = \lim_{\tau\to 0}\widetilde{U}_{\theta(e,i)} = -\frac{3\sqrt{2}\lambda_{\theta(e,i)}}{1+\xi}\tau^{1/2}\sin\theta\ \text{ierfc}\ u_{e,i}^0 \tag{16b}$$

It is to be noted that the convective term in the left hand side of Eq. (9) involves only the radial component of the flow field. It reduces here to $\widetilde{U}_{r(e,i)}^0(\partial\overline{T}_{e,i}^0/\partial y)$ and is easily derived from Eqs. (13a), (13b) and (16a) Then, writing $\widetilde{T}_{e,i}^{(0)} = \lim_{\tau\to 0}\widetilde{T}_{e,i}$, and searching at solutions expressed in a dimensionlesss form:

$$\frac{\widetilde{T}_e^{(0)}}{T_0 - T_\infty} = \frac{\sqrt{2}\lambda_{T_e}}{(1+\beta)(1+\xi)}\cos\theta\tau^{3/2}F_e(w_e^0) \tag{17}$$

$$\frac{\widetilde{T}_i^{(0)}}{T_0 - T_\infty} = \frac{\beta}{1+\beta}\frac{\sqrt{2}\lambda_{T_i}}{(1+\xi)}\cos\theta\tau^{3/2}F_i(w_i^0) \tag{18}$$

in which the $\lambda_{T(e,i)}$ parameters are defined as:

$$\lambda_{T_e} = \sqrt{\frac{Pr_e}{Re_e}}, \quad \lambda_{T_i} = \sqrt{\frac{Pr_i}{Re_e}} \tag{19}$$

we get a new differential equation verified by the functions $F_e(w_e^0)$ and $F_i(w_e^0)$ as follows:

$$F''(Z) + 2ZF'(Z) - 6F(Z) = \Phi(Z) \tag{20}$$

Denoting z as the variable $z = Z/\sqrt{Pr}$, the right hand side in (20) is defined as:

$$\Phi(Z) = K\exp(-Z^2)\Psi(z) \tag{21a}$$

$$\Psi(z) = i^2\text{erfc}\ z - \frac{1}{4} \tag{21b}$$

These formulas hold both for the external and internal problem, with in each case:

$$K = K_e = +\frac{48}{\sqrt{\pi}}, \quad Z = w_e^0, \quad z = u_e^0, \tag{22}$$

$$K = K_i = -\frac{48}{\sqrt{\pi}}, \quad Z = w_i^0, \quad z = u_i^0 \tag{23}$$

The homogeneous equation $F''(Z) + 2ZF'(Z) - 6F(Z) = 0$ possesses well known solutions [4], denoted here as $F_h(Z)$, which are linear combinations of i^3erfc Z and i^3erfc $(-Z)$ functions. We will retain here the only one which is a fast decreasing function:

$$F_h(Z) = C\ i^3\text{erfc}\ Z \tag{24}$$

Making use of (24), a particular solution of the full Eq. (20) may be found, applying twice the method based on the variation of constants. For instance, a fast decreasing solution, which vanishes as $Z \to 0$ reads:

$$F_p(Z) = -i^3\mathrm{erfc}\ Z \times \int_0^Z \mathrm{d}x \frac{\exp -x^2}{(i^3\mathrm{erfc}\ x)^2} \times \int_x^\infty \mathrm{d}y\ \Phi(y)\ i^3\mathrm{erfc}\ y \tag{25}$$

This solution is a function of Z and it depends also on the Prandtl numbers (Pr_e or Pr_i) through $\Phi(y)$ (cf. Eqs. (21a) and (21b)). Its practical evaluation requires however double quadratures. We find it better to calculate $F_p(Z)$ (at least a part of it) as an expansion on a set of orthogonal Hermite polynomials. The method is detailed in Appendix A . Recalling that z stands for $Z/\sqrt{Pr}$ we get from Eq. (A.18):

$$F_p(Z) = \frac{K}{32}\mathrm{e}^{-Z^2}\left[1 - \mathrm{erfc}\ z\left(1 + \frac{1}{3Pr} + \frac{4}{3}z^2\right) - \frac{16}{\sqrt{\pi}}\mathrm{e}^{-z^2}\sum_{p\geqslant 0}\sigma_p H_{2p+1}\left(\sqrt{1+Pr}z\right)\right] \tag{26}$$

The H_n's stand here for the (odd) Hermite polynomials, and the σ_p denotes the coefficients of the above-mentioned expansion. Their expressions are given explicitly in (A.15a), (A.15b) and (A.16). Let us just remark that as $\sigma_p \sim \sigma_1(1/2Pr)^{p-1}$ for $p \geqslant 1$, the polynomial expansion in the right hand side of (26) is nothing but an expansion in successive powers of $(1/2Pr)$. In the case of liquids, this number is lower than unity for most of them. [2] Collecting together (24) and (26), this allows us to express finally the temperature distributions (17) and (18) as:

$$\frac{\widetilde{T}_\mathrm{e}^{(0)}}{T_0 - T_\infty} = \frac{\sqrt{2}\lambda_{T_\mathrm{e}}}{(1+\beta)(1+\xi)}\cos\theta\tau^{3/2}F_\mathrm{e}(w_\mathrm{e}^0) \tag{27}$$

$$\frac{\widetilde{T}_\mathrm{i}^{(0)}}{T_0 - T_\infty} = \frac{\beta}{(1+\beta)}\frac{\sqrt{2}\lambda_{T_\mathrm{i}}}{(1+\xi)}\cos\theta\tau^{3/2}F_\mathrm{i}(w_\mathrm{i}^0) \tag{28}$$

with explicitly:

$$F_{\mathrm{e,i}}(w_{\mathrm{e,i}}^0) = C_{\mathrm{e,i}}\, i^3\mathrm{erfc}\ w_{\mathrm{e,i}}^0 + F_{p(\mathrm{e,i})}(w_{\mathrm{e,i}}^0) \tag{29}$$

In (29), the two constants C_e and C_i, which factorize the homogeneous solutions have to be deduced from the conditions at the interface (See Section 4). Also the notation $F_{p(\mathrm{e,i})}$ has been used for $F_p(Z)$ according to whether $Z = w_\mathrm{e}^0$ or $Z = w_\mathrm{i}^0$, and $Pr = Pr_\mathrm{e}$ or $Pr = Pr_\mathrm{i}$ within $z = Z/\sqrt{Pr}$ in expression (26).

[2] It is possible however to express the polynomial expansion in the right hand side of (26) in a different way, namely as $\sum_p s_p H_{2p+1}(z)$ in which the s_p's are now functions of the parameter $\delta = (1/(1+Pr)) > 1$. This ensures the convergence of the expansion whatever the value of Pr. These mathematical derivations will not be presented in the present work.

4. Initial and boundary conditions. Conditions at the interface

Owing to the initial and boundary conditions fulfilled by Chao's solutions [3], (Eqs. (1a) and (1b)), which hold also for (13a) and (13b), the initial and boundary conditions for the droplet velocity and viscid thermal distributions $\widetilde{T}_\mathrm{e}(y,\theta,t)$ and $\widetilde{T}_\mathrm{i}(y,\theta,t)$ (Eqs. (27) and (28)) read:

$$\begin{array}{ll} t<0, & t>0 \\ U=0, & U=U_\infty \\ y<0, & y>0 \\ \widetilde{T}_\mathrm{i}(y,\theta,0)=0, & \widetilde{T}_\mathrm{e}(y,\theta,0)=0 \\ \widetilde{T}_\mathrm{i}(-\infty,\theta,t)=0, & \widetilde{T}_\mathrm{e}(\infty,\theta,t)=0 \\ \dfrac{\partial\widetilde{T}_\mathrm{i}}{\partial\theta}(y,0,t)=0, & \dfrac{\partial\widetilde{T}_\mathrm{e}}{\partial\theta}(y,0,t)=0 \\ \dfrac{\partial\widetilde{T}_\mathrm{i}}{\partial\theta}(y,\pi,t)=0, & \dfrac{\partial\widetilde{T}_\mathrm{e}}{\partial\theta}(y,\pi,t)=0 \end{array} \tag{30}$$

The first four conditions on the thermal profiles are readily ensured due to the fact that for $t \to 0$ or $|y| \to \infty$, it comes $w_{\mathrm{e,i}}^0 \to \infty$, and that (27) and (28) are fast decreasing functions. The conditions on the derivatives $(\partial\widetilde{T}_{\mathrm{e,i}}/\partial\theta) = 0$ when $\theta = 0$ or $\theta = \pi$ are also automatically ensured as the angulaire dependence is only contained within the explicit $\cos\theta$ term.

The conditions at the interface:

$$\widetilde{T}_\mathrm{e}(0,\theta,t) = \widetilde{T}_\mathrm{i}(0,\theta,t) \tag{31}$$

$$k_\mathrm{e}\frac{\partial\widetilde{T}_\mathrm{e}}{\partial y}(0,\theta,t) = k_\mathrm{i}\frac{\partial\widetilde{T}_\mathrm{i}}{\partial y}(0,\theta,t) \tag{32}$$

lead to

$$\sqrt{Pr_\mathrm{e}}F_\mathrm{e}(0) = \beta\sqrt{Pr_\mathrm{i}}F_\mathrm{i}(0) \tag{33}$$

$$\sqrt{Pr_\mathrm{e}}F_\mathrm{e}'(0) = -\sqrt{Pr_\mathrm{i}}F_\mathrm{i}'(0) \tag{34}$$

which provides

$$C_\mathrm{e} = \frac{1}{\sqrt{Pr_\mathrm{e}}}\frac{A+\beta B}{1+\beta}, \quad C_\mathrm{i} = \frac{1}{\sqrt{Pr_\mathrm{i}}}\frac{B-A}{1+\beta} \tag{35}$$

The coefficients A and B in (35) are equal to:

$$A = -6\sqrt{\pi}\left[\sqrt{Pr_\mathrm{e}}F_{p\mathrm{e}}(0) - \beta\sqrt{Pr_\mathrm{i}}F_{p\mathrm{i}}(0)\right] \tag{36a}$$

$$B = 4\left[\sqrt{Pr_\mathrm{e}}F_{p\mathrm{e}}'(0) + \sqrt{Pr_\mathrm{i}}F_{p\mathrm{i}}'(0)\right] \tag{36b}$$

From (26), one can check that:

$$F_{p\mathrm{e}}(0) = -\frac{K_\mathrm{e}}{96Pr_\mathrm{e}} = -\frac{1}{2\sqrt{\pi}Pr_\mathrm{e}}, \quad F_{p\mathrm{i}}(0) = -\frac{K_\mathrm{i}}{96Pr_\mathrm{i}} = +\frac{1}{2\sqrt{\pi}Pr_\mathrm{i}} \tag{37}$$

which gives for A the following simple expression:

$$A = 3\left[\frac{1}{\sqrt{Pr_e}} + \frac{\beta}{\sqrt{Pr_i}}\right] \tag{38}$$

The exact calculation of the derivative $F'_p(Z=0)$ is given in Appendix A (Eq. (A.20)). Taking into account of (22) and (23) one gets:

$$\begin{aligned} F'_{pe}(0) &= \frac{K_e}{16\sqrt{\pi}}\Xi(Pr_e) \equiv \frac{3}{\pi}\Xi(Pr_e), \\ F'_{pi}(0) &= \frac{K_i}{16\sqrt{\pi}}\Xi(Pr_i) \equiv -\frac{3}{\pi}\Xi(Pr_i) \end{aligned} \tag{39}$$

where the function $\Xi(Pr)$ is defined by Eq. (A.21). This yields finally for B (Eq. (36b)) the following result:

$$B = \frac{12}{\pi}\left[\sqrt{Pr_e}\Xi(Pr_e) - \sqrt{Pr_i}\ \Xi(Pr_i)\right] \tag{40}$$

It should be appreciated that the numerical coefficients A and B given in Eqs. (38) and (40) are simple functions of the Prandtl numbers Pr_e and Pr_i. The required C_e and C_i coefficients are directly derived from Eq. (35), and similarly to A and B, they depend only on Pr_e and Pr_i.

Finally, Chao's solutions for the thermal distributions (1a) and (1b), corrected of viscid effects according to (8a) in the short time limit read:

$$\frac{T_e - T_\infty}{T_0 - T_\infty} = \frac{1}{1+\beta}\left(\operatorname{erfc} w_e + \frac{1}{1+\sqrt{\frac{\mu_i\rho_i}{\mu_e\rho_e}}}\sqrt{\frac{2Pr_e}{Re_e}}\cos\theta\,\tau^{3/2}F_e(w_e^0)\right) \tag{41a}$$

$$\frac{T_i - T_\infty}{T_0 - T_\infty} = 1 - \frac{\beta}{1+\beta}\left(\operatorname{erfc} w_i - \frac{1}{1+\sqrt{\frac{\mu_i\rho_i}{\mu_e\rho_e}}}\sqrt{\frac{2\ Pr_i}{Re_e}}\cos\theta\,\tau^{3/2}F_i(w_i^0)\right) \tag{41b}$$

Rigorously in that limit, the arguments of the erfc functions in the Chao's solutions would have to be taken as w_e^0 and w_i^0 (cf Eq. (14)). However, for practical and numerical applications, it is better to retain the exact expressions for w_e and w_i (Eq. (2)) in order to get the right angular and time dependence detailed explicitly in (3)–(5).

5. Numerical application and discussion

In what follows, we apply the formalism detailed above to the case where the dispersed phase is made of organic droplets, namely *n*-pentane and carbon tetrachloride, plunged in a surrounding homogeneous medium which consists of water at 20 °C. The initial temperature of the droplet has been taken as 30 °C for *n*-pentane, and 70 °C for carbon tetrachloride, practically near below their boiling point (36.1 and 76.5 °C respectively). Numerical datas for the liquids are given in Table 1. For further numerical considerations, let us recall that viscid contributions (27) and (28) were derived under a number of limitating hypotheses: (a) a thin boundary layer approximation, (b) a perturbative scheme, (c) the shape of droplet kept fixed with time, and (d) a short time analysis. Condition (a) implies that Reynolds numbers are sufficiently large namely $\frac{|y|}{R} \ll \frac{1}{\sqrt{Re}}$ where $|y|$ is of the order of the hydrodynamic boundary layer thickness. With, say $|y| \lesssim \frac{R}{5}$, it yields $Re \gg 25$ for the smallest of Re_e and Re_i, namely Re_e in the present case. So, one can retain as a *very lower* bound $Re_e \gtrsim 40$–50. Condition (b) is fulfilled until the λ_T expansion parameters (19) are sufficently small which means $Re_e \gg \sup(Pr_e, Pr_i)$. For the actual values of the Prandtl numbers Pr_e and Pr_i (see Table 1), it turns that condition (b) is already fulifilled when condition (a) applies. [3] Condition (c) implies that the viscosity of the liquid droplets and the interfacial tension σ are sufficiently large to prevent modification of their spherical shape, by damping inertial and gravitational effects. This yields an upper bound on the internal Reynolds number [1] $Re_i \lesssim 500$. However, it must be noted at this stage that viscid contributions (27) and (28) get fully negligible when the Reynolds numbers exceed typically two hundred. Thus our results hold practically within the range $50 \lesssim Re_e \lesssim 200$. A condition for the interfacial tension σ can be derived through the capillarity constant $a = (2\sigma/\rho_i g)^{1/2}$ of the liquid droplet. [4] This yields an upper bound on its radius $R_{max} \lesssim a$. For the organic liquids considered in the present study, their interfacial tension with water [7] is of order 50 mN/m. This makes R_{max} to be of order 0.5 cm. The interfacial tension also enters in the expression of droplet frequency oscillations [8], with a squared minimum frequency given by $\omega_{min}^2 = (8\sigma/\rho_i R^3)$. Then, it follows that on average, the droplet will remain nearly spherical as it moves if $(U_\infty/R) \ll \omega_{min}$, which yields a condition on the Weber number $(2R\rho_i U_\infty^2/\sigma) \ll 16$. Practically it has been shown [9] that if the Weber number is less than 4, droplets would exhibit only little oscillations. Thus, for a given radius, the droplet velocity U_∞ must not be too large otherwise oscillations due to capillarity will affect its shape. We can write this condition as $U_\infty \lesssim (\sigma/\nu_e Re_e \rho_i)$,

[3] It should be noted that this condition is less restrictive that the constraint of a thin boundary thermal layer approximation $(|y|/R) \ll (1/\sqrt{Pe})$.

[4] Strictly speaking, the capillarity constant of a liquid involves its surface tension against air.

Table 1
Numerical data for the liquids at 20 °C used in our numerical application (see Section 5)

	n-pentane	Carbon tetrachloride	Water
ρ (kg/m^3)	626.2	1593.4	998.23
μ (mPa s)	0.235	1.0584	1.002
ν (10^{-6} m^2/s)	0.372	0.664	1.004
Pr	3.922	8.325	7.133
k (W/m K)	0.136	0.1078	0.5876
c_p (J/g K)	2.270	0.848	4.1819
κ (m^2/s)	0.0957	0.0798	0.1408

With these values the parameters β and ξ defined in the nomenclature are found to be equal to 3.56 and 0.38 for *n*-pentane in water and to 4.10 and 1.30 for carbon tetrachloride in water, respectively.

which practically gives U_∞ lower than a few cm/s. For instance, for a droplet of carbon tetrachloride in water, with $Re_e = 100$, we get $U_\infty \lesssim 30$ cm/s and then, $R \gtrsim 0.15$ mm. Looking now at condition d) with say, $\tau \lesssim 0.3$ as a *very large* upper limit for the dimensionless time variable, it comes for instance with $U_\infty = 2$ cm/s, $R = 2.5$ mm (which corresponds to $Re_e = 100$), $t \lesssim 37.5$ ms for the true time variable. Finally, it should be noted that thermal viscid distributions (27) and (28) were derived with the underlying hypothesis that the physical properties of the liquids remain constant. This hypothesis is valid provided that dissipation is sufficiently small. It is known from the 1930's that impulsively generated flows around a body are initially inviscid. It follows that at short time, the boundary layers on both sides of the interface are very thin and viscous dissipative terms $\sim\nu\Delta\widetilde{U}$ in the Navier–Stokes equation are large only in that region. However, as is shown below, thermal distributions remain practically unaffected by these viscous effects in the interfacial region. Consequently, refinements to account for the variation of physical constants may be no longer justified.

Hermite polynomials in the expansion of the $F_p(Z)$ function (Eq. (26)) have been computed up to $p = 10$, on a grid with a scale $\delta z = 0.01$, in the dimensionless variable $z = \frac{y}{R}$ within the range $(-0.5, +0.5)$. In the present case, values for the upper coefficients σ_p in the polynomial expansion were found to be $\sim 10^{-20}$ for the external problem and $\sim 10^{-18}$ for the internal one. Also various values for the external Reynolds number with $Re_e \geqslant 40$, the dimensionless time τ with $\tau \geqslant 0.01$, and the θ angle have been retained.

Fig. 2 exhibits a plot of the internal and external thermal distributions in the case $Re_e = 40$, $\tau = 0.3$ at $\theta = 30°$. For this rather weak value of the Reynolds number, the expansion parameters λ_T (19) are large and equal to $\lambda_{T_e} = 0.423$ for water and $\lambda_{T_i} = 0.313$ for *n*-pentane and $\lambda_{T_i} = 0.456$ for carbon tetrachloride respectively. Despite this fact, the viscid corrections are small and the thermal distributions remain very closed to that of Chao. Similar results hold for other values of the θ angle and, obviously, for larger value of the Reynolds number and/or smaller values of τ, due to the occurrence of the $\tau^{3/2}/\sqrt{Re_e}$ factor in the expressions (41a) and (41b). Also , it is to be noted that these viscid corrections do not really affect the interface (i.e., the region located at $y = 0$), but they develop in the adjacent boundary layers.

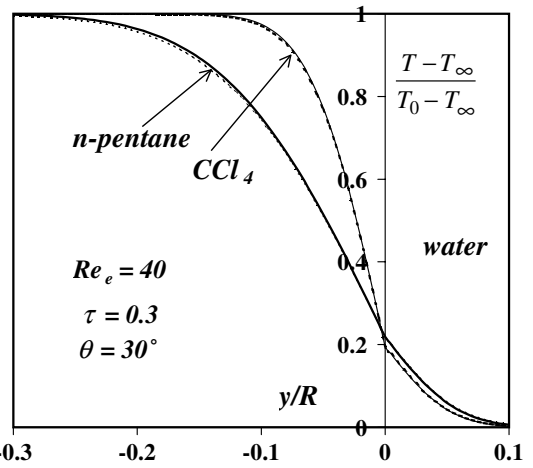

Fig. 2. Comparison of the reduced thermal distributions including viscid effects (dot lines), computed from Eqs. (41a) and (41b), with the inviscid solutions by Chao [3] in the case of droplets of *n*-pentane and carbone tetrachloride moving in water.

The very small contribution of viscid effects to the thermal distributions at the interface is due to the weak value of the $F_{e,i}(w^0_{e,i})$ functions at $y = 0$, which are of order $\sim 10^{-2}$. This result itself is a consequence of the numerical value of B (Eq. (40)) which can be shown to be necessarily weak. Indeed, for large enough Prandtl numbers, a feature which actually holds (see Table 1), one gets from Eq. (A.21):

$$\Xi(Pr) \approx \frac{8}{5}Pr^{-1/2} + \frac{12}{35}Pr^{-3/2} + \cdots \tag{42}$$

and then from (40), $B \approx 0$, which implies:

$$C_e \approx \frac{3}{1+\beta}\left(\frac{1}{Pr_e}+\frac{\beta}{\sqrt{Pr_e Pr_i}}\right) \quad \text{and}$$
$$C_i \approx -\frac{3}{1+\beta}\left(\frac{1}{\sqrt{Pr_e Pr_i}}+\frac{\beta}{\sqrt{Pr_i}}\right) \tag{43}$$

The values of $F_{e,i}(0)$ are directly derived as:

$$F_e(0) = \frac{C_e}{6\sqrt{\pi}} + F_{pe}(0) \approx \frac{1}{2\sqrt{\pi}}\frac{\beta}{1+\beta}\left(\frac{1}{\sqrt{Pr_e Pr_i}}-\frac{1}{Pr_e}\right) \tag{44a}$$

$$F_i(0) = \frac{C_i}{6\sqrt{\pi}} + F_{pi}(0) \approx \frac{1}{2\sqrt{\pi}}\frac{1}{1+\beta}\left(\frac{1}{Pr_i}-\frac{1}{\sqrt{Pr_e Pr_i}}\right) \tag{44b}$$

They are at least as small as the Prandtl numbers are large. A similar conclusion is achieved if Pr_e and Pr_i are not necessarily large but they have the same order of magnitude, as is the case for instance for water and carbon tetrachloride liquids. Indeed, let us consider the particular case where $Pr_e = Pr_i$. Then it follows from (37) that $F_{pe}(0) = -F_{pi}(0)$, and from (40) that $B \equiv 0$. This implies from (35) that $C_e = -C_i$, and finally $F_e(0) = -F_i(0)$. This is compatible with the condition at the interface (33) only if $F_e(0) = F_i(0) = 0$. Consequently, at least in the small time limit, the viscid effects will not have a great importance on the thermal distributions at the interface, compared to that of Chao. It remains to analyze these effects in the two adjacent internal and external boundary layers. Apart the weight factor $\tau^{3/2}/\sqrt{Re_e}$, viscid contributions are closely linked to the behavior of the functions $F_e(w_e^0)$ and $F_i(w_i^0)$ which are first the relevant quantities to analyze. Fig. 3 exhibits a plot of these functions in the case of a droplet of *n*-pentane, [5] with $Re_e = 100$, at three different times, $\tau = 0.05$, 0.10 and 0.15. It clearly features that viscid contributions are negligible at the interface, as previously stated. Also we note the spreading of these regions with increasing time. These features are reproduced in a similar manner by the full viscid thermal distributions (27) and (28), which are ploted in Fig. 4, in the case of a hot droplet of carbon tetrachloride ($\theta = 70$ °C) in water at 20 °C, with $Re_e = 50$, at three different times, $\tau = 0.1$, 0.2 and 0.3. Together with the above mentioned spreading effect, they also exhibit a quick increase with time as a consequence of the $\tau^{3/2}$ factor. Also, it is to be noted that viscid corrections to thermal distributions are most significant in the liquid droplet than in the surrounding liquid. This is partly due to the occurrence of the β coefficient ($\beta = 3.56$ and 4.10 for *n*-pentane and

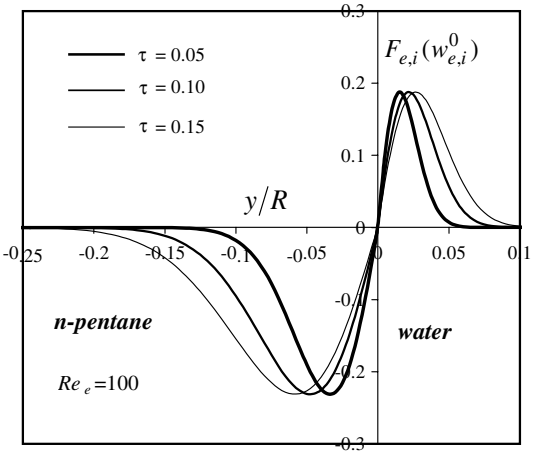

Fig. 3. Plot of the functions $F_{e,i}(w^0_{e,i})$ according to Eq. (29), supplemented with Eqs. (26) and (14) as a function of the dimensionless variable y/R, in the case of an oil droplet of *n*-pentane moving in water.

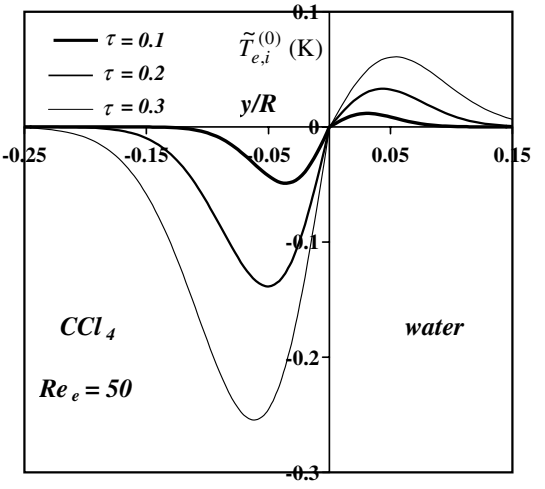

Fig. 4. Plot of the viscid thermal distributions $\tilde{T}^0_{e,i}$ given by Eqs. (27) and (28), as a function of the dimensionless variable y/R, in the case of an organic droplet of *n*-pentane at $\theta = 70$ °C moving in water at $\theta = 20$ °C.

carbontetrachloride against water respectively) which enter in the expression of $\tilde{T}^{(0)}_i$. The spreading effect can be explained by the analytical form of the functions $F_{e,i}(w^0_{e,i})$ which are fast decreasing function of the dimensionless variable (14), while the behavior at the interface arises from the conditions (33) and (34). Let us finally mention that for most cases the absolute maximal value of these functions (see Fig. 3) is ~0.2. This leads to absolute contributions of order ~0.1–0.3 K (see Fig. 4) for the viscid thermal distributions which remain obvi-

[5] It should be noted that functions $F_{e,i}(w^0_{e,i})$ depend on the nature of both the internal and external liquids, but not of their temperature.

ously small in the range of applicability of our study, i.e. large Reynolds and Peclet numbers to ensure the thin boundary layer approximation, and short time analysis. It must be stressed however that if the thermal viscid distributions $\sim\tau^{3/2}F_{e,i}(0)$ are small, this is no longer the case of the heat flux $\sim\tau^{1/2}F'_{e,i}(0)$, even at short time, which is a very important feature.

6. Conclusion

In this work, we have studied the effect of viscosity on the thermal transfer at and on both sides of a spherical interface associated with a translating liquid droplet moving at constant velocity in another liquid of infinite extent at rest. Calculations of the thermal internal and external distributions have been done along a perturbative scheme valid in the thin boundary layer approximation. Exact algebraic solutions have been derived in the small time limit. For a part of them, they are expressed as power series of Hermite polynomials. A numerical application to a concrete case of an organic droplet of *n*-pentane and carbon tetrachloride moving in water has been performed. It follows from this study that the transient thermal distributions are pratically not disturbed at the interface, by comparison to the inviscid distributions. However, this feature hold no longer for the heat flux. Viscous effects on the thermal transfer are shown on the contrary to occur preferably on both side of the interface, in the two adjacent boundary layers, with a stronger effect for the liquid droplet. We are planning to extend our study to the evaluation of transient thermal distributions at any time and also to investigate the case where the droplet radius is not kept fixed.

Appendix A. Rsolution of Eq. (20)

In this Appendix, we give the calculation of a particular solution of differential equation (20). For a part of it, it is based on an expansion on a set of Hermite polynomials. For the sake of simplicitly, mathematical details will be omitted and only the main steps of the method of resolution will be exposed. As in the main text the variable z will stand for $Z/\sqrt{Pr}$.

First the i^2erfc z function in the right hand side of Eq. (20) is rewritten as a combination of the erfc z and $\exp(-z^2)$ functions, which leads to [4]:

$$F''(Z)+2ZF'(Z)-6F(Z)=\frac{K}{4}\left((1+2z^2)\mathrm{erfc}\ z-\frac{2}{\sqrt{\pi}}z\exp(-z^2)-1\right)\exp(-Z^2) \tag{A.1}$$

The search of a particular solution $F_p(Z)$ may be done splitting it in a first step as $F_p=F_0+F_1+F_2$ where F_0 is the solution of the following equation:

$$F_0''(Z)+2ZF_0'(Z)-6F_0(Z)=-\frac{K}{4}\exp(-Z^2) \tag{A.2}$$

which immediately provides:

$$F_0(Z)=\frac{K}{32}\exp(-Z^2) \tag{A.3}$$

Next, the $F_1(Z)$ function is calculated in order to eliminate the complementary error function erfc z in the right hand side of Eq. (A.1). For that purpose, $F_1(Z)$ is written as $F_1(Z)=\Psi_1(Z)\mathrm{erfc}\ z$, with $\Psi_1(Z)$ such that:

$$\Psi_1''(Z)+2Z\Psi_1'(Z)-6\Psi_1(Z)=\frac{K}{4}(1+2z^2)\exp -Z^2 \tag{A.4}$$

This yields

$$\Psi_1(Z)=(a+bZ^2)\exp -Z^2$$

with

$$a=-\frac{K}{32}\left(1+\frac{1}{3Pr}\right)\quad\text{and}\quad b=-\frac{K}{24Pr} \tag{A.5}$$

and finally

$$F_1(Z)=-\frac{K}{32}\exp(-Z^2)\mathrm{erfc}\ z\left(1+\frac{1}{3Pr}+\frac{4}{3}z^2\right) \tag{A.6}$$

Then the differential equation the remaining $F_2(Z)$ function obeys is derived as:

$$F_2''(Z)+2ZF_2'(Z)-6F_2(Z)=-\frac{K}{2\sqrt{\pi}}\mathrm{e}^{-(Z^2+z^2)}(\alpha z+\beta z^3) \tag{A.7}$$

with

$$\alpha=\left(\frac{3}{4}+\frac{1}{3Pr}-\frac{1}{12Pr^2}\right)\quad\text{and}\quad\beta=-\left(\frac{1+Pr}{3Pr}\right) \tag{A.8}$$

So the right hand side in (A.7) contains no longer any complementary error function but an exponential factorized by an odd polynomial.

The problem is now to find a particular solution of Eq. (A.7). In a first step we carry out the change of variable $Y=\sqrt{Z^2+z^2}$, and we note now $G(Y)$ for $F_2(Z)$. Next, through the change of function $G(Y)=-(K/2\sqrt{\pi})\mathrm{e}^{-Y^2}S(Y)$, Eq. (A.7) is transformed as a new differential equation on $S(Y)$. Reexpressing in its right hand side $\alpha z+\beta z^3$ as a linear combination of the Hermite polynomials $H_1(Y)$ and $H_3(Y)$, and rearranging terms in its left hand side, gives after a number of algebraic manipulations:

$$[S''(Y) - 2YS'(Y) - 8S(Y)] + Pr^{-1}[S'' - 4YS' - 2S(1-2Y^2)] = A_1H_1(Y) + A_3H_3(Y) \quad (A.9)$$

In the right hand side of (A.9), the coefficients A_1 and A_3 are functions of Pr defined as:

$$A_1 = \frac{1}{\sqrt{1+Pr}}\left(\frac{3}{8} - \frac{1}{12Pr} - \frac{1}{24Pr^2}\right) \quad (A.10a)$$

$$A_3 = -\frac{1}{24}\frac{1}{Pr\sqrt{1+Pr}} \quad (A.10b)$$

At this stage, we proceed to the afore-mentioned polynomial expansion, expanding $S(Y)$ in a power series on a basis of (odd) Hermite polynomials:

$$S(Y) = \sum_{n\,\text{odd}} s_n H_n(Y) \quad (A.11)$$

Making use of the differential equation the H_n's obey and taking account of a number of their recurrence formulas [10], one gets from (A.9) and (A.11) the following result:

$$-\sum_n (8+2n)s_nH_n(Y) + Pr^{-1}\sum_n s_nH_{n+2}(Y) = A_1H_1(Y) + A_3H_3(Y) \quad (A.12)$$

The following recurrence formulas are directly deduced from this equation, identifying each polynomial contribution:

$$s_1 \equiv -\frac{A_1}{10} \quad (A.13a)$$

$$s_3 = -\frac{1}{14}\left(A_3 - \frac{s_1}{Pr}\right) = -\frac{1}{14}\left(A_3 + \frac{1}{10Pr}A_1\right) \quad (A.13b)$$

$$s_n = \frac{1}{Pr}\frac{s_{n-2}}{8+2n} \quad \text{for } n \geqslant 5 \quad (A.13c)$$

As $S(Y)$ in (A.11) is expanded on a set of odd Hermite polynomials, we are entitled to write $n = 2p+1$ which leads finally to:

$$S(Y) = \sum_{p\geqslant 0} \sigma_p H_{2p+1}(Y) \quad (A.14)$$

with

$$\sigma_0 = s_1 = -\frac{A_1}{10} = -\frac{1}{240}\frac{1}{\sqrt{1+Pr}}\left(9 - \frac{2}{Pr} - \frac{1}{Pr^2}\right) \quad (A.15a)$$

$$\sigma_1 = s_3 = -\frac{1}{14}\left(A_3 + \frac{1}{10Pr}A_1\right) = \frac{1}{3360}\frac{1}{\sqrt{1+Pr}}\left(\frac{1}{Pr} + \frac{2}{Pr^2} + \frac{1}{Pr^3}\right) \quad (A.15b)$$

The resolution of the recurrence formula (A.13c) is straightforward, and leads to the simple result:

$$\sigma_p \equiv \left(\frac{1}{2Pr}\right)^{p-1}\frac{7!!\sigma_1}{(2p+5)!!} \quad \text{for } p \geqslant 2 \quad (A.16)$$

It is important to note that the numerical value of the coefficients σ_p decreases very quickly, practically by a factor 10 at each time. This allows to truncate the series (A.14) to a few number of terms for its numerical evaluation.

Gathering all these results, we get for $F_2(Z)$ the closed expression:

$$F_2(Z) = G(Y) = -\frac{K}{2\sqrt{\pi}}e^{-(Z^2+z^2)}\sum_{p\geqslant 0}\sigma_pH_{2p+1}(\sqrt{Z^2+z^2}) \quad (A.17)$$

and, adding Eqs. (A.3), (A.6) and (A.17), the overall expression of a particular solution of Eq. (20)

$$F_p(Z) = \frac{K}{32}e^{-Z^2}\left[1 - \operatorname{erfc} z\left(1 + \frac{1}{3Pr} + \frac{4}{3}z^2\right) - \frac{16}{\sqrt{\pi}}e^{-z^2}\sum_{p\geqslant 0}\sigma_pH_{2p+1}\left(\sqrt{Z^2+z^2}\right)\right] \quad (A.18)$$

In order to evaluate the C_e and C_i coefficients (cf. Eqs. (35)) from Eqs. (36a) and (36b), the value of this function and that of its derivative at the origin must be calculated. Evaluation of $F_p(0)$ is straightforward:

$$F_p(0) = -\frac{K}{96Pr} \quad (A.19)$$

The derivative $F_p'(0)$ is derived directly from (A.18) as:

$$F_p'(0) = \frac{K}{16\sqrt{\pi}}\Xi(Pr) \quad (A.20)$$

with

$$\Xi(Pr) = \left(1 + \frac{1}{3Pr}\right)\sqrt{\frac{1}{Pr}} - 8\sqrt{\frac{1+Pr}{Pr}}\Sigma(Pr) \quad (A.21)$$

In the last expression, $\Sigma(Pr)$ corresponds to the value at the origin of the term by term derivative of the polynomial expansion given in Eq. (A.14):

$$\Sigma(Pr) = \sum_{p\geqslant 0}\sigma_p(Pr)H'_{2p+1}(0) = 2\sigma_0(Pr) + \sum_{p\geqslant 1}(-1)^p2^{p+1}(2p+1)(2p-1)!!\sigma_p(Pr) \equiv 2\sigma_0(Pr) - 4\ 7!!\sigma_1(Pr)\sum_{p\geqslant 1}\left(\frac{-1}{Pr}\right)^{p-1}\frac{(2p+1)!!}{(2p+5)!!} \quad (A.22)$$

The study of the remaining series in (A.22) leads, for $Pr > 1$, to the result [11]:

$$\Sigma(Pr) = 2\sigma_0(Pr) - 2\ 7!!\sigma_1(Pr)\left\{ \frac{2}{15}Pr + (Pr^{5/2} + Pr^{7/2})\text{Arc tg}\sqrt{\frac{1}{Pr}} - \frac{2}{3}Pr^2 - Pr^3 \right\} \tag{A.23a}$$

It should be noted that this formula can be also found starting from the integral expression (25). Moreover, in that case, it can be proved that it holds for $Pr < 1$ as well.

References

[1] R. Clift, J.R. Grace, M.E. Weber, Bubbles, Drops and Particles, Academic Press, New York, 1978.

[2] C. Pozrikidis, Introduction to the Theoretical and Computational Fluid Dynamics, Oxford University Press, 1997.

[3] B.T. Chao, J. Heat Transfer, Trans. ASME 273 (1969) 273–281.

[4] Abramowitz, Stegun, Handbook of Mathematical Functions, ninth ed., Dover Publications, Inc., New York, 1970.

[5] L.M. Milne-Thomson, Theoretical Hydrodynamics, fourth ed., The MacMillan Company, New York, 1960.

[6] R. Askovic, Académie Royale de Belgique, Bulletin de la Classe des Sciences, série 6 tome XI (2000) 367–375.

[7] A.W. Adamson, Physical Chemistry of Surfaces, John Wiley and Sons, New York, 1990.

[8] L. Landau, E. Lifchitz, Physique Théorique, Tome VI: Mécanique des Fluides. Editions MIR, Moscou, 1971.

[9] S. Winnikow, B.T. Chao, Phys. Fluids 9 (1966) 50.

[10] I.S. Gradshteyn, I.M. Ryzhik, Table of Integrals, Series and Products, fourth ed., Academic Press, New York, 1965.

[11] E.R. Hansen, A Table of Series and Products, Prentice-Hall, Inc., Englewood Cliffs, NJ, 1975.